Adsorption and Desorption of Methanol on Pd (111) and on a Pd/V Surface Alloy

R. Schennach,*,† A. Eichler,‡ and K. D. Rendulic†

Institute of Solid State Physics, Graz University of Technology, Austria, and Institut für Materialphysik & Center for Computational Materials Science, Universität Wien, Sensengasse 8/12, A-1090 Vienna, Austria

Received: August 7, 2002; In Final Form: October 15, 2002

The adsorption and subsequent dissociation reaction of methanol on Pd (111) has been the focus of several studies due to the importance of this reaction as a model for the production of methanol from hydrogen and carbon monoxide. While the question, whether the C−O bond of adsorbed methanol on Pd (111) can be opened, has been settled recently, there is no experimental proof for the mechanistic explanation of this reaction pathway. By combination of thermal desorption spectroscopy and density functional theory we present evidence that a hydrogen bond between two neighboring methanol molecules on the Pd (111) surface is necessary to break the C−O bond. A complete suppression of the C−O bond cleavage in methanol is possible by changing the electronic structure of the surface due to the formation of a Pd/V surface alloy. The same result can be achieved by using a molecular beam of methanol with a high translational energy. This effect is explained in terms of dissociative adsorption via C−H bond scission at high methanol energies instead of molecular methanol adsorption.

Introduction

Adsorption and subsequent reaction of methanol on single-crystal surfaces has been studied by a number of groups.[1−14] The system is of interest not only for a basic understanding of the adsorption and desorption of small organic molecules on single-crystal surfaces but also for the petrochemical industry. The production of methanol from syngas ($CO + H_2$) is an important reaction for the petrochemical industry. ZnO/Cr_2O_3 mixed oxides and Cu supported on ZnO, Cr_2O_3, and Al_2O_3 have been used as catalysts for this reaction. It has been shown that Pd supported on silica is a very active and selective catalyst for methanol synthesis.[15] This spurred more detailed studies on the adsorption and reaction of methanol on palladium surfaces.[16−23]

Many catalytic processes are carried out over supported bimetallic catalysts. It has been shown that bimetallic surfaces can exhibit significantly different chemical and catalytic properties than either monometallic component.[24] The observed changes are explained either by modifications of the electronic structure of the surface upon alloying, or by different types of active sites. The combination of a reactive (V) and a noble (Pd) transition metal is characterized by significant differences in d-band occupation. Such alloys show a strong chemical interaction between the unlike atoms arising from d−d hybridization. A unique alloy is formed when V is deposited on Pd, as the V atoms end up in the second atomic layer only. Therefore one has the same first atomic layer and the same bulk as in Pd (111) which means that V leads only to a change in the electronic structure of the surface.[24]

The question if the C−O bond in methanol can be broken on the Pd (111) surface was discussed in detail a couple of years ago by the group of Winograd.[5] They showed that the C−O bond is only broken if the methanol coverage on the surface is close to one monolayer, i.e., just before the multilayer shoulder/peak in the thermal desorption spectra starts to grow. Starting from this methanol coverage adsorbed on the palladium surface at about 100 K, the main reaction is the desorption of methanol at a temperature of about 170 to 220 K (∼75%). From the remaining 25% on the Pd surface the largest part becomes dehydrogenated, resulting finally in CO and H_2, which desorb at about 480 and 320 K, respectively. For a small fraction of methanol molecules, an opening of the C−O bond occurs by the formation of water from the reaction of two neighboring adsorbed methanol molecules forming a methoxy and a methyl species on the surface ($2CH_3OH \rightarrow CH_3O + CH_3 + H_2O$). The methoxy dehydrogenates further, while the methyl either reacts with adsorbed hydrogen to form methane (which desorbs around 250 K) or dehydrogenates to amorphous carbon. A hydrogen bridge between the two methanol molecules was proposed as the driving force for the CO-bond scission.[5]

In this paper, we provide strong experimental evidence that a hydrogen bridge between two neighboring methanol molecules is indeed necessary for the C−O bond cleavage. Further, we present a structural model for such a dense methanol layer on the Pd surface on the basis of DFT calculations. Increasing the kinetic energy inhibits the formation of such a structure (and hence CO bond scission) due to dissociative adsorption via C−H bond breaking ($E_{act} = 0.41$ eV). On the alloyed Pd/V surface, the lower reactivity leads to a complete suppression of C−O bond opening, in agreement with the calculated adsorption and activation energies.

Experimental Section

The experiments were done in a supersonic molecular beam apparatus described previously.[25] The UHV chamber was equipped with an AES, a rotateable quadrupole mass spectrometer (goniometer configuration), an electron beam evaporator, and a quartz microbalance for monitoring the evaporating flux. For all our experiments the nozzle was kept at room temperature,

* Author to whom correspondence should be addressed at Graz University of Technology, Institute of Solid State Physics, Petersgasse 16/2, 8010 Graz, Austria. E-mail: robert.schennach@tugraz.at.

† Graz University of Technology.

‡ Universität Wien.

10.1021/jp021841q CCC: $25.00
Published on Web 02/25/2003

yielding a measured translational energy of 105 meV for methanol. Higher translational energies (250 meV) were achieved by seeding the methanol beam in He. The given translational energies are mean energies obtained from the analysis of time-of-flight measurements. The time-of-flight data indicate a rather wide energy distribution because of the low stagnation pressure of methanol (133 mbar). Thermal desorption experiments were done—after adsorption at 100K—with a heating rate of 4 K s^{-1}, and the desorbing molecules were detected with the multiplexed quadrupole mass spectrometer.

The Pd (111) crystal had a surface area of about 0.71 cm^2 and was cleaned following a procedure described earlier.[26] The cleanliness of the surface was checked by Auger Electron Spectroscopy (AES). To produce the Pd/V surface alloy, 0.3 ML of vanadium (with respect to the number of palladium atoms in the first layer) were deposited on the crystal using the electron beam evaporator with a deposition rate of 0.1 ML min^{-1}. The Pd crystal was kept at 573 K during V deposition. At this temperature the V is transferred into the second layer, forming a subsurface alloy. This process was described in detail elsewhere.[27]

After attaching the glass vial with the methanol (Chromasolv, Riedel-de Haën) to the gas inlet system for the molecular beam source, the methanol was further cleaned by several freeze-and-thaw cycles. To create a supersonic molecular beam the vapor pressure of methanol at room temperature (133 mbar[28]) was sufficient.

Computational

Structures and binding energies have been calculated using the Vienna ab initio Simulation Package (VASP).[29−31] VASP is a plane-wave-based density functional code employing the projector augmented wave method.[32] For further computational details, we refer to ref 33 where the structure of the Pd/V alloy has been investigated using the same method. The surface has been modeled by a four-layer slab in a $p(2\sqrt{3}\times\sqrt{3})$ cell containing 6 atoms per layer, sampled by a grid of $(3 \times 6 \times 1)$ k-points. A cutoff energy for the expansion of the plane waves of 400 eV was found to be sufficient for an accurate description. For exchange and correlation generalized gradient corrections (GGA) according to Perdew et al.[34] have been applied. Transition states have been calculated using the nudged elastic band method.[35] Frequencies have been obtained by diagonalization of the dynamical matrix from finite displacements ($\Delta = \pm 0.02$ Å) of every ion of the adsorbates into each Cartesian coordinate.

Experimental Results

For all experiments methanol was adsorbed at a surface temperature of 100 K by exposing the crystal to the molecular beam. Different amounts of methanol on the surface were achieved by varying the exposure time. During our desorption experiments we were able to reproduce the reaction pattern described in ref 5 and in the Introduction. We found desorption peaks for methanol (mass 31, which is the main peak in the mass spectrum of methanol[36]), hydrogen (mass 2), CO (mass 28), and in case of a full monolayer of methanol before desorption, a CH_4 peak (mass 16).

Desorbing water from the C−O bond cleavage reaction could not be detected. This is due to the fact that the water desorption temperature[37] coincides with the methanol desorption temperature on the Pd (111) surface and mass 18 is a rather large fragment of methanol in the mass spectrum of methanol.[36] Therefore the C−O bond opening was followed via the methane signal (mass 16), which is detected at a higher temperature,

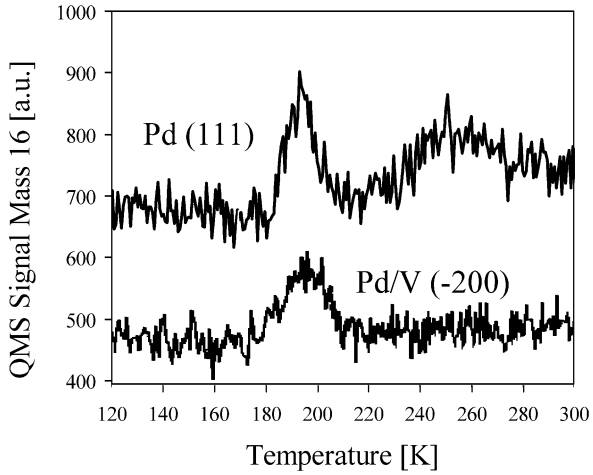

Figure 1. Desorption of methanol from Pd (111) (upper curve) and Pd/V (lower curve). Mass 16, heating rate 4 K s^{-1}. The initial coverage was one monolayer of methanol. For clarity we subtracted 200 au from the mass 16 signal in the lower curve.

where the methanol is already completely desorbed. The mass 16 signal as a function of temperature after adsorption of one monolayer methanol is shown in Figure 1. The pronounced peak for the Pd (111) surface (upper curve) at around 195 K is the mass 16 fragment of the methanol desorption peak. The smaller broad peak at about 252 K is due to methane desorption. The second thermal desorption spectrum (lower curve) shown in Figure 1 was obtained from the Pd/V alloy surface. Again there is a mass 16 signal as a fragment from the desorption of methanol around 195 K. However, there is no mass 16 signal from methane desorption corresponding to the 250 K peak for the pure Pd surface. The surface alloy completely inhibits the C−O bond opening independent of the initial methanol coverage. It has already been shown before that the Pd/V alloy is less reactive than the clean Pd surface.[24,26] A similar trend in reactivity was found for methanol adsorption on Pt and Pt/Sn surface alloys.[38]

Figure 2a shows the mass 28 signal, where a significant shift from 486 K at the Pd (111) surface to 440 K on the alloy surface of the CO peak can be seen. The CO peak due to the dehydrogenation reaction of methanol behaves like the CO peaks after CO adsorption.[24,26] This is not surprising, as all the other products from methanol dehydrogenation are already completely desorbed, when CO desorption starts. The small shoulder for CO desorption from the alloy at around 480 K is due to CO desorption from the (vanadium-free) backside of the crystal.[24,26] For hydrogen (Figure 2b), a similar shift to lower desorption temperatures can be observed going from clean Pd (111) (peak maximum at 318 K) to the Pd/V surface alloy (peak maximum at 295 K). The temperatures at the desorption peak maxima are the same as in the case of pure hydrogen adsorption.[26] Apparently the coadsorbed CO does not influence the hydrogen desorption, suggesting no lateral interactions between adsorbed H and CO under these experimental conditions.

One cannot stop the dehydrogenation reaction after the first hydrogen was abstracted by simply heating the sample. The onset temperatures of the different dehydrogenation steps are too close. Therefore experiments with the He-seeded beam were done to achieve dissociative adsorption of methanol at 100 K due to the increased translational energy. Only at the highest translational energy that can be reached by seeding methanol with He with the nozzle at room temperature (250 meV), a significant effect was found. Higher translational energies could be reached by heating the nozzle, but at elevated temperature

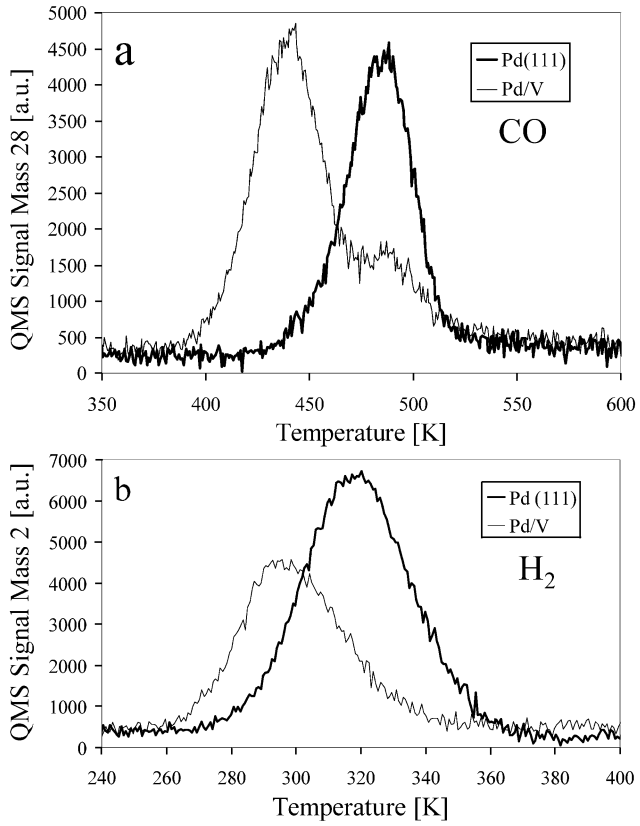

Figure 2. Desorption of methanol from Pd (111) (thick line) and Pd/V (thin line). (a) Mass 28, and (b) mass 2, heating rate 4 K s^{-1}.

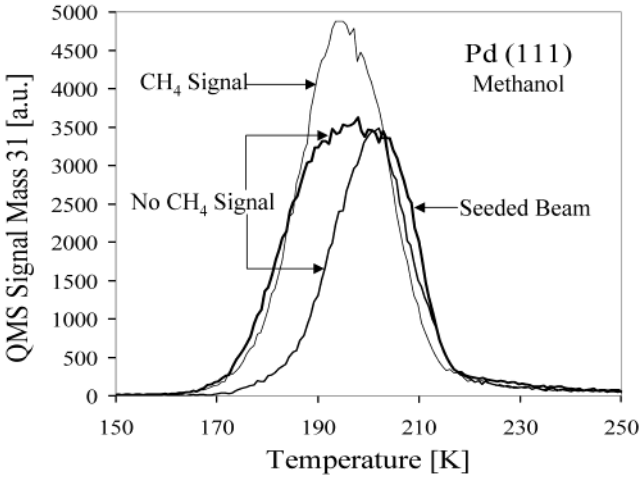

Figure 3. Desorption of methanol from Pd (111), mass 31, heating rate 4 K s^{-1}. Broad peak: methanol adsorbed with He-seeded beam (E_{trans} = 250 meV) one monolayer methanol (thick line). Two different methanol surface concentrations after pure methanol adsorption (E_{trans} = 105 meV). Highest peak: 1 ML of methanol (thin line). Smallest peak: less than 1 ML of methanol (thicker line).

the methanol reacts on the surface of the nozzle, which is made of Mo. The influence of the translational energy of the methanol beam is shown in Figures3 and 4 for the clean Pd (111) surface and for the Pd/V surface alloy, respectively. On the clean Pd (111) surface (Figure 3) one can see a marked difference in the methanol desorption peaks (mass 31) after adsorption of one monolayer of methanol at low translational energy (E_{trans} = 105 meV) and after adsorption of one monolayer at high translational energy (E_{trans} = 250 meV). The highest peak at 194 K (thin line), which corresponds to a full monolayer of methanol adsorbed with the pure methanol beam, is associated with a

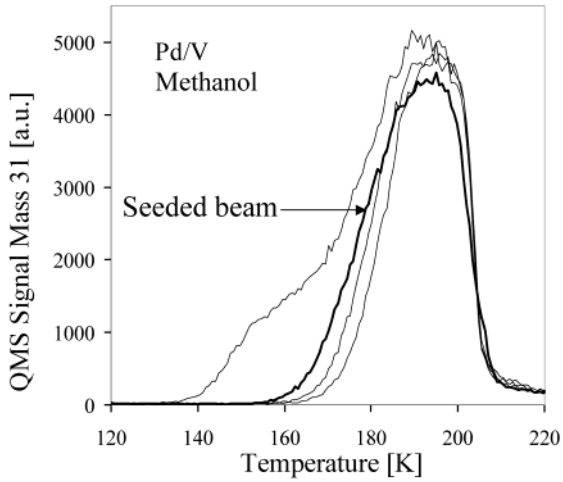

Figure 4. Desorption of methanol from Pd/V, mass 31, heating rate 4 K s^{-1}. Thick line indicated by the arrow: One monolayer of methanol adsorbed with He-seeded beam (E_{trans} = 250 meV). Thin lines: Different initial methanol surface concentrations after pure methanol adsorption (E_{trans} = 105 meV).

methane signal. The smallest peak at 202 K, which corresponds to less than one monolayer coverage (adsorbed with E_{trans} = 105 meV), is not associated with a methane peak (thicker line). This is in agreement with previous work.[5] The broad peak centered around 197 K (thick line), which corresponds to a full monolayer of methanol adsorbed from the He-seeded beam (E_{trans} = 250 meV), seems to be a superposition of the two other peaks, with slightly different intensity ratios. In this case there is no methane production detectable. Independent of the methanol coverage, we were never able to detect a methane signal after adsorption from the seeded beam.

Experiments with the seeded beam on the alloy surface lead to a different result. As can be seen from Figure 4, there is no effect of adsorption with increased beam energy (thick line in Figure 4) on the desorption peaks of methanol (mass 31) with the same initial coverage from the Pd/V alloy surface. The temperature at the peak maximum is 195 K, so there is no significant shift in the methanol desorption temperature going from clean Pd (111) to the Pd/V alloy. As mentioned earlier we did not find any methane production on the alloy surface (compare to Figure 1).

DFT Calculations

For a further investigation of this system ab initio calculations were performed. The adsorption site and geometry of methanol (Figure 5a) and several possible fragments (Figure 5b) have been optimized. The corresponding adsorption energies are compiled in Table 1.

While the saturated molecules (methanol (Figure 5a), water (Figure 5b)) and the methyl and hydroxymethyl group (Figure 5b) prefer the on-top geometry, all others adsorb in higher coordinated sites. With the exception of hydrogen on the Pd−V alloy occupying the hcp-hollow above the V atom ("hcp-V"), all other fragments adsorb in (or in the case of methoxy close to) fcc hollow sites.The methoxy is shifted toward the bridge position so that the methyl group over the hcp-V position can come closer to the surface. Similarly also OH tilts toward this hcp-V site. Adsorption of formaldehyde (Figure 5b) is exceptional: the two hydrogen atoms make the carbon isoelectronic to oxygen, resulting in a di-σ configuration with two comparable bonds to the substrate.

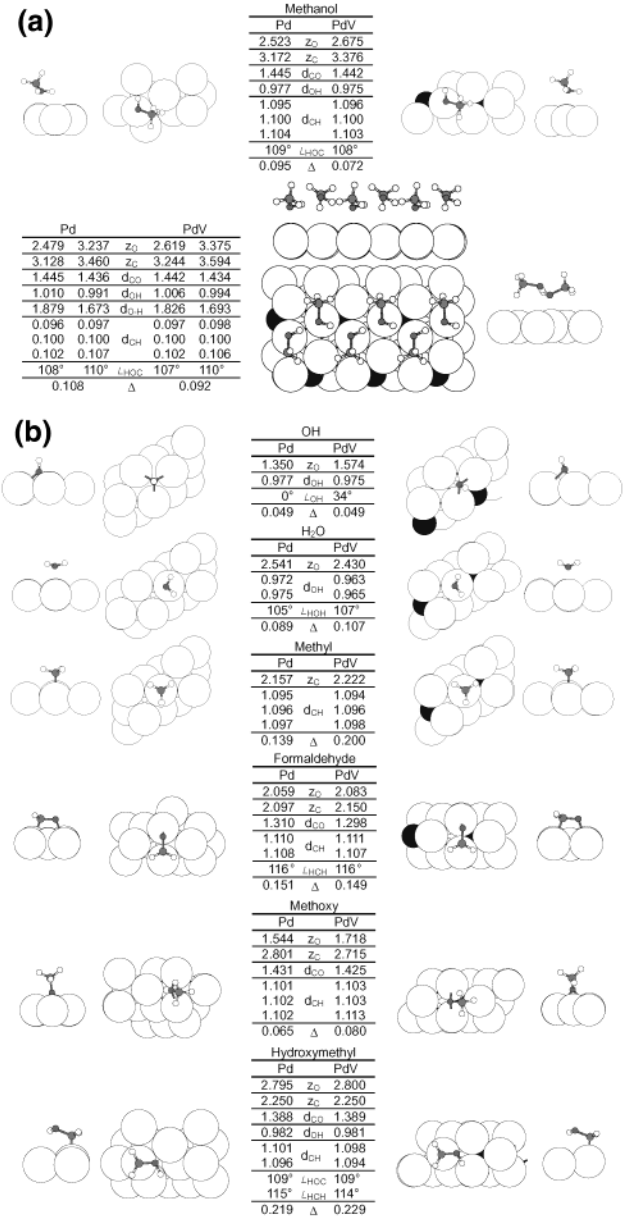

Figure 5. (a) Sketches of methanol, and (b) some possible fragments (OH, H_2O, CH_3, CH_2O, CH_3O, CH_2OH) on a Pd (111) surface (left column) and on a Pd−V subsurface alloy (right column), as obtained from ab initio calculations. Pd and V are represented by large white and black disks, respectively; hydrogen, carbon, and oxygen by small white, light-gray, and dark-gray disks, respectively. The tables in the middle summarize the most important structural parameters: heights above the average surface plane *z*, bond lengths *d* (in Å), and bond angles *L*. The last line in the table (Δ) gives the buckling (Δ = max-(z_{Pd}) − min(z_{Pd})) of the first substrate layer in Å. The panel at the bottom of (a) describes the high-coverage methanol structure. Since the structure is very similar on both surfaces, only the adsorption on the alloy is shown, in the table both structures are described.

Comparing the geometries over the Pd (111) surface and the alloy all molecules are closer to the surface for the pure metal and also the elongation of the bonds is more pronounced, reflecting the higher reactivity of the pure Pd surface.[26] The first indicators for this lower reactivity of the alloy are of course the lower adsorption energies (see Table 1).

A somewhat special geometry was found for the high coverage structure with two methanol molecules per ($\sqrt{3}\times 2\sqrt{3}$) unit cell (one molecule per three Pd atoms) shown in Figure 5a. In this high-density bilayer structure the methanol molecules are close enough to form hydrogen bonds. While the adsorption

TABLE 1: Methanol and Various Fragments on Pure Pd (111) and on a Pd−V Subsurface Alloy[a]

		Pd (111)		Pd/V	
adsorbate	reference	site	energy	site	energy
CH_3OH	CH_3OH	top(O)	0.32	top(O)	0.24
$2\times CH_3OH$	$2\times CH_3OH$	top(O)	0.51	top(O)	0.47
CH_3O	CH_3OH-H^*	bridge(O)	0.12	bridge(O)	−0.24
CH_2OH	CH_3OH-H^*	top(C)	0.54	top(C)	−0.00
CH_2O	CH_2O	di-σ (C,O)	0.63	di-σ (C,O)	0.42
	$CH_3OH-2\times H^*$	di σ (C,O)	0.60	di σ (C,O)	0.01
CH_3	CH_3OH-OH^*	top(C)	0.01	top(C)	−0.38
	CH_4-H^*	top(C)	0.05	top(C)	−0.44
H_2O	H_2O	top(O)	0.25	top(O)	0.10
OH	H_2O-H^*	fcc(O)	0.10	fcc(O)	−0.21
H	$0.5\times H_2$	fcc	0.69	hcp-V	0.49

[a] The adsorption energies (in eV; no zero-point corrections applied) are given with respect to the reference structure in the second column (the asterisk denotes adsorbed species). The atoms in brackets after the adsorption site specify which atom bonds (predominantly) to the surface.

geometry of the first methanol molecule is very similar to the low coverage case, the second molecule is oriented such that the methyl groups disturb each other least and the oxygen atoms can efficiently be connected via hydrogen bonds. So the second-layer methanol molecules are above the first ones ($\Delta z_O = \sim 0.8$ Å; $\Delta z_C = \sim 0.3$ Å) with the methyl group rotated by ∼180° and the hydrogen at the hydroxyl group pointing down, establishing the connection to the next molecule. In that manner, neighboring molecules form chains which are linked by hydrogen bonds alternating between 1.88 (1.83) and 1.67 (1.69) Å on the pure metal (alloy) surface (Figure 5a). This stabilization due to hydrogen bonds results also in a substantial increase of the adsorption energy per molecule (compare to Table 1) of 0.19 eV (on the alloy even 0.23 eV). The formation of a "second layer" at this coverage indicates that we are already close to saturation coverage, i.e., further methanol adsorption will result in true multilayer growth. So it is probable, that the monolayer coverage defined via the shape of the TPD spectra (compare to Figure 4, highest curve) is (at least) very similar to this bilayer structure. A similar structure is well-known as the so-called bilayer structure of water adsorbed on metal surfaces, which consists of a chemisorbed first layer and a second layer with 2 or 3 hydrogen bonds to the first layer.[39]

For the discussion of bond-scission, the potential energies for methanol adsorbed in various modifications (isolated molecules, after O−H scission, after C−O scission, high-coverage phase) are summarized in Figure 6. For all coadsorption structures the interaction between neighboring molecules has been neglected (i.e., $E(A + B) = E(A) + E(B)$, for two fragments A, B), except for the high coverage methanol structure with two molecules per unit-cell (compare to Figure 5a). Also included in Figure 6 are the activation energies for C−O, C−H, and O−H bond-breaking. While the breaking of the CO bond requires more than 1.5 eV (starting from adsorbed methanol even almost 2 eV), the C−H and O−H bonds are weaker, as expected.

Another factor that lowers the activation energy for the breaking of the hydrogen bonds quite significantly is zero-point energies. These have been obtained on the basis of the calculated frequency spectra ν_i via $\Delta E = 0.5\Sigma h\nu_i$, with *h* being Planck's constant. The absence of the high-energy C/O−H stretch-frequency at the transition state leads to a decrease of the barrier by about 150 meV. The lowest activation energy is connected with the C−H scission leading to hydroxymethyl, in agreement

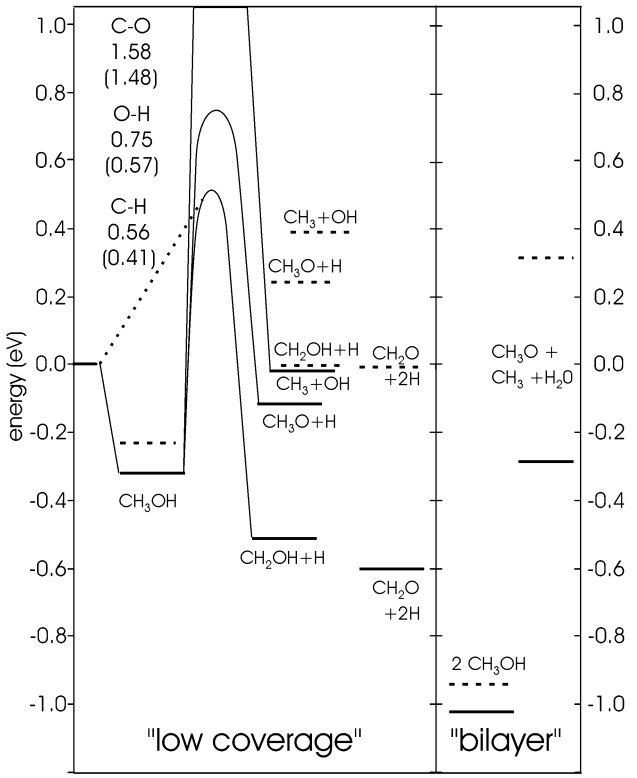

Figure 6. Energy diagram for the first bond scission (C−H, O−H, or C−O bond) of methanol on Pd (111) (full lines) and a Pd−V subsurface alloy (dashed lines) with respect to the gas-phase methanol molecule, as obtained from ab initio calculations. The values next to the transition states are the potential energies at the barrier. The number in brackets gives the zero-point energy corrected value. A dotted line indicates a direct dissociative adsorption from the gas phase. The left-hand side shows the low coverage case with one methanol molecule per $p(2\sqrt{3}\times\sqrt{3})$ cell, the right-hand side the hydrogen bond stabilized high coverage structure with two methanol molecules per $p(2\sqrt{3}\times\sqrt{3})$ cell.

with the findings for Pt (111) in ref 3. We will come back to the C−H vs O−H bond breaking in the Discussion section.

On the less reactive alloy surface, the "final states" after the first bond-scission are significantly higher in energy (~0.4−0.5 eV). Under the assumption, that the transition states behave similarly to the final states (which can be expected, since all three bond breakings occur via late transition states; compare to Figure 7), the barriers for bond breaking on the Pd−V alloy will be significantly higher than those on the pure surface. We checked this for the (presumably lowest) barrier to C−H cleavage, which we calculated to be 0.78 eV with respect to the gas-phase (before zero-point correction).

In the high coverage configuration the final state after C−O (and O−H) bond breaking is more favorable, due to the formation of three adsorbate−metal bonds (water, methyl, and methoxy) after the reaction. This could enable the C−O bond breaking for this bilayer structure. Again, for the alloy, such a reaction would be highly endothermic (compared to desorption).

Discussion

Combining the results from the TPD experiments and the ab initio simulations a consistent picture of methanol adsorption/desorption/dissociation can be drawn. At low temperature (100 K), methanol can adsorb molecularly via the oxygen atom with an adsorption energy of 0.32 eV. Upon heating, most of the methanol desorbs, resulting in mass 16 and mass 31 signals at around 200 K (Figures 1 and 3). About 25% of the methanol dehydrogenates, resulting finally in H_2 and CO desorbing from

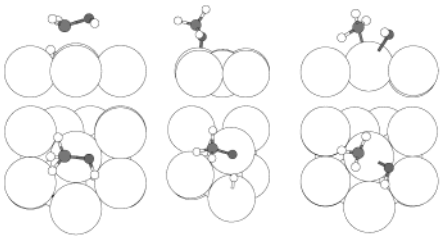

	C-H	O-H	C-O
z_O	2.831	2.150	2.012
z_C	2.435	2.861	2.426
z_H	1.145	1.186	2.149
d_{CO}	1.390	1.419	1.937
d_{OH}	0.981	1.717	0.984
d_{CH}	1.485	1.105	1.091
	1.098	1.104	1.125
	1.093	1.113	1.087
$\angle_{HOC}$	109°	122°	99°
Δ	0.132	0.149	0.329

Figure 7. Sketches for the transition states of C−H, O−H, and C−O bond breaking of methanol on a Pd (111) surface. Pd atoms are represented by large white disks; hydrogen, carbon, and oxygen by small white, light-gray, and dark-gray disks, respectively. The table summarizes the most important structural parameters: heights above the average surface plane *z*, bond lengths *d* (in Å), and bond angles *L*. The last line in the table (Δ) gives the buckling ($\Delta = \max(z_{Pd}) - \min(z_{Pd})$) of the first substrate layer in Å.

the surface at 295 and 486 K, respectively. According to the DFT calculations, this dehydrogenation process is initiated by C−H bond cleavage ($E_{act} = 0.41$ eV) and the formation of a hydroxymethyl species. Although it was generally assumed in the past that the first bond-cleavage results in a methoxy species,[5−7,10,12,13] there are already in the literature some hints for hydroxymethyl. First, in secondary ion mass spectrometry[5,14] of isotopically labeled methanol, never CH_3O^+ or CD_3O^+ but CH_2OD^+ and CH_2OH^+ could be detected; second, in an electron energy loss spectroscopy study, Davis and Barteau[12] found an intense peak at 705 cm^{-1} after methanol adsorption at 170 K. This peak cannot be explained by methanol or methoxy species (compare to Figure 8). However, a frustrated rotation (around the C−O axis) in the spectrum of hydroxymethyl has a calculated frequency of 694 cm^{-1}.

Adsorption of more methanol results in the formation of a bilayer structure (Figure 5a), which is stabilized by hydrogen bonds. These strong hydrogen bonds can lead (for a small fraction of the adsorbates) to the reaction of two methanol molecules forming methyl, methoxy, and a water molecule (Figure 6, right part). Methyl recombines with hydrogen from the surface and desorbs as methane detected as a mass 16 signal around 250 K (Figure 1). Water already desorbs earlier at about the same temperature as methanol, so that the mass 18 signal is shadowed by the mass 18 fragment of methanol desorption. The methoxy dehydrogenates further and desorbs as CO and H_2.

Adsorption with the seeded beam and hence higher kinetic energy results to some extent in the dissociative adsorption of methanol via C−H bond cleavage. This suppresses the formation of the bilayer structure and in consequence the C−O bond scission. The dissociation barrier ($E_{act} = 0.41$ eV, compared to the dotted line in Figure 6) could be overcome by some methanol molecules of the rather wide energy distribution of our seeded beam experiments, as the measured translational energy of 0.25 eV is the mean energy calculated from the actually measured flight time distribution. This dissociative adsorption can also explain the different desorption peak shapes

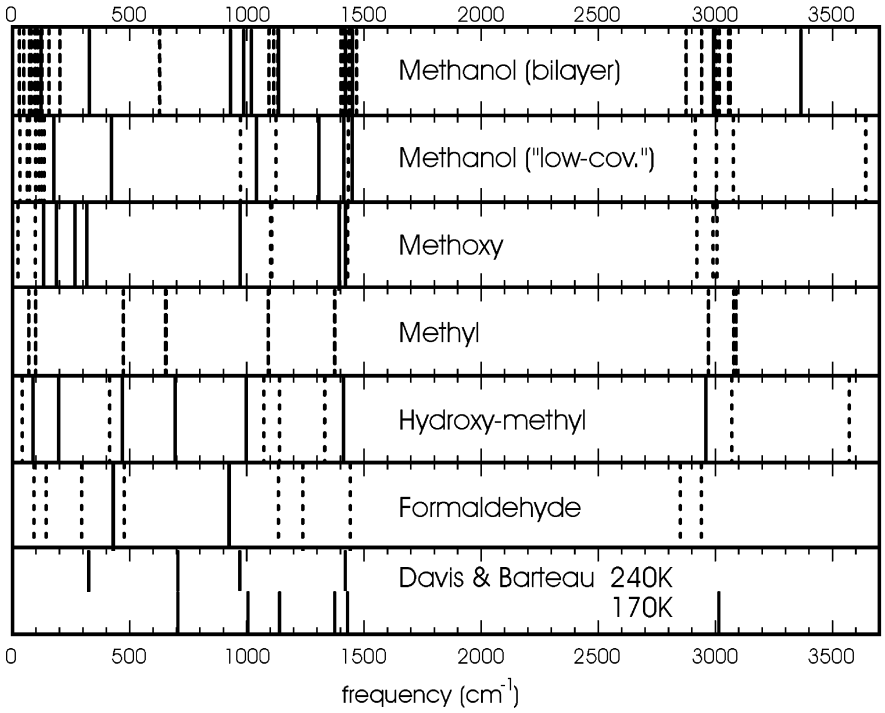

Figure 8. Calculated frequency spectra for methanol and some possible stable intermediates during dissociation. Modes with a large dynamic dipole moment are indicated by full lines, modes with a rather small dynamic dipole moment are dashed. For comparison, experimental electron energy loss spectroscopy results from ref 12 are shown in the bottom panel for heating of a methanol layer to $T = 170$ K (lower half) and $T = 240$ K (upper half).

after adsorption with pure methanol (highest peak in Figure 3) and adsorption with He seeding (broad peak in Figure 3).

The alloyed surface is generally less reactive, as already shown in the past for CO and H_2 adsorption, due to the downshift of the d-band caused by the alloyed vanadium.[24,38] Although the structure of the first layer is identical to that of the pure Pd (111) surface,[27] adsorption energies are much smaller (Table 1 and Figure 6) at almost identical geometries (Figure 5a,b). So the higher translational energy is too small to overcome the barrier for dissociative adsorption on the alloy surface. Therefore the shape of the desorption peaks for pure methanol adsorption and adsorption from the seeded beam is similar (Figure 4). The bilayer structure can be formed (the hydrogen bond is even slightly stronger than on the pure surface), but the adsorption of the products (after CO cleavage and the split-off of water) is highly endothermic. Consequently, no methane signal can be detected from the alloy surface.

Summary

Methanol adsorbs at 100 K on both Pd (111) and on the Pd/V surface alloy. During desorption, about 25% of the adsorbed methanol undergoes reaction via O−H bond cleavage, ultimately forming CO and H_2. On the pure surface at about one monolayer methanol coverage, a bilayer structure stabilized by hydrogen bonds can be formed. Thus C−O bond cleavage (of a small fraction of molecules) is possible, leading to methane formation. On the Pd/V alloy surface the latter reaction pathway is not possible as a result of the different electronic structure of the alloy surface. The calculated geometries for Pd (111) and for the Pd/V alloy are very similar, which also suggests that the differences between the two surfaces are due to electronic effects rather than steric effects.

Adsorption of methanol with higher translational energy leads to complete suppression of the C−O bond cleavage reaction, since methanol under these conditions adsorbs partially dissociatively via C−H bond cleavage. So the bilayer structure, which is necessary for CO bond opening, cannot be formed.

Our experiments and calculations are an indirect proof that the formation of hydrogen-bonded methanol chains on the Pd (111) surface, together with energetically favorable adsorption states of the initial reaction products (methyl and hydroxyl), are necessary for C−O bond scission.

Acknowledgment. This work was supported by the Austrian "Fonds zur Förderung der wissenschaftlichen Forschung" Project S 8102-Phy which is part of the joint project "Gas Surface Interactions".

References and Notes

(1) Solymosi, F.; Tarnóczi, T. I.; Berkó, A. *J. Phys. Chem.* **1984**, *88*, 6170.
(2) Endo, M.; Matsumoto, T.; Kubota, J.; Domen, K.; Hirose, C. *J. Phys. Chem. B* **2000**, *104*, 4916.
(3) Desai, S. K.; Neurock, M.; Kourtakis, K. *J. Phys. Chem. B* **2002**, *106*, 2559.
(4) Solymosi, F.; Berkó, A.; Tarnóczi, T. I. *Surf. Sci.* **1984**, *141*, 533.
(5) Chen, J.-J.; Jiang, Z.-C.; Zhou, Y.; Chakraborty, B. R.; Winograd, N. *Surf. Sci.* **1995**, *328*, 248.
(6) Rebholz, M.; Matolin, V.; Prins, R.; Kruse, N. *Surf. Sci.* **1991**, *251/252*, 1117.
(7) Rebholz, M.; Kruse, N. *J. Chem. Phys.* **1991**, *95* (10), 7745.
(8) Street, S. C.; Liu, G.; Goodman, D. W. *Surf. Sci.* **1997**, *385*, L971.
(9) Kok, G. A.; Noordermeer, A.; Nieuwenhuys, B. E. *Surf. Sci.* **1983**, *135*, 65.
(10) Kruse, N.; Rebholz, M.; Matolin, V.; Chuah, G. K.; Block, J. H. *Surf. Sci.* **1990**, *238*, L457.
(11) Parmeter, J. E.; Jiang, X.; Goodman, D. W. *J. Vac. Sci. Technol.* **1991**, *A 9* (3), 1810.
(12) Davis, J. L.; Barteau, M. A. *Surf. Sci.* **1990**, *235*, 235.
(13) Zhang, C. J.; Hu, P. *J. Chem. Phys.* **2001**, *115*, 7182.
(14) Levis, R. J.; Zhicheng, J.; Winograd, N. *J. Am. Chem. Soc.* **1989**, *111*, 4605.
(15) Poutsma, M. L.; Elek, L. F.; Ibarbia, P. A.; Risch, A. P.; Rabo, J. A. *J. Catal.* **1978**, *52*, 157.
(16) Jorgensen, S. W.; Madix R. J. *Surf. Sci.* **1987**, *183*, 27.
(17) Holroyd, R. P.; Bowker, M. *Surf. Sci.* **1997**, *377/379*, 786.

(18) Hartmann, N.; Esch, F.; Imbihl, R. *Surf. Sci.* **1993**, *297*, 175.
(19) Solymosi, F.; Berkó, A.; Tóth, Z. *Surf. Sci.* **1993**, *285*, 197.
(20) Kito, T.; Eberhart, M. E. *Surf. Sci.* **1996**, *357/358*, 609.
(21) Francis, S. M.; Corneille, J.; Goodman, D. W.; Bowker, M. *Surf. Sci.* **1996**, *364*, 30.
(22) Bhattacharya, A. K.; Chesters, M. A.; Pemble, M. E.; Sheppard, N. *Surf. Sci.* **1988**, *206*, L845.
(23) Bowker, M.; Holroyd, R. P.; Sharpe, R. G.; Corneille, J. S.; Francis, S. M.; Goodman, D. W. *Surf. Sci.* **1997**, *370*, 113.
(24) Beutl, M.; Lesnik, J. *Surf. Sci.* **2001**, *482/485*, 353.
(25) Berger, H. F.; Rendulic, K. D. *Surf. Sci.* **1991**, *253*, 325.
(26) Beutl, M.; Lesnik, J. *Vacuum* **2001**, *61*, 113.
(27) Konvicka, C.; Jeanvoine, Y.; Lundgren, E.; Kresse, G.; Schmid, M.; Hafner, J.; Varga, P. *Surf. Sci.* **2000**, *463*, 199.
(28) *CRC Handbook of Chemistry and Physics*, 55th ed.; CRC Press: Cleveland, OH, 1974−1975.
(29) Kresse, G.; Furthmüller, J. *Phys. Rev. B* **1996**, *54*, 11169.
(30) Kresse, G.; Furthmüller, J. *Computat. Mater. Sci.* **1996**, *6*, 15.
(31) http://cms.mpi.univie.ac.at/vasp/
(32) Kresse, G.; Joubert, D. *Phys. Rev. B* **1998**, *59*, 1758.
(33) Hirschl, R.; Jeanvoine, Y.; Kresse, G.; Hafner, J. *Surf. Sci.* **2001**, *482*, 712.
(34) Perdew, J. P.; Chevary, J. A.; Vosko, S. H.; Jackson, K. A.; Pederson, M. R.; Singh, D. J.; Fiolhais, C. *Phys. Rev. B* **1992**, *46*, 6671.
(35) Mills, G.; Jónsson, H.; Schenter, G. K. *Surf. Sci.* **1995**, *324*, 305.
(36) EPA/NIH Mass Spectral Data Base, Vol. 1; U.S. Government Printing Office, Washington, DC, 1978.
(37) He, J.-W.; Norton, P. R. *Surf. Sci.* **1990**, *238*, 95.
(38) Hammer, B.; Morikawa, Y.; Norskov, J. K. *Phys. Rev. Lett.* **1996**, *76*, 2141.
(39) Thiel, P. A.; Madey, T. E. *Surf. Sci. Rep.* **1987**, *7*, 211.